[16th Global Congress on Manufacturing and Management GCMM 2022]

Additive manufacturing of hygromorphic structures using regenerated cellulose/PLA biocomposites

Christian Gauss[a1], Kim Pickering[a], Maxime Barbier[b], Tim Miller[c]

[a] *School of Engineering, The University of Waikato, Private Bag 3105, Hamilton, New Zealand*
[b] *Scion, Materials, Engineering and Manufacturing group, Private Bag 3020, Rotorua 3010, New Zealand*
[c] *School of Design Innovation, Victoria University of Wellington, PO Box 600, Wellington, New Zealand*

Abstract

Three-dimensional printing technologies are at the forefront of the current industrial revolution, enabling the production of complex shapes using a wide range of materials without relying on large production facilities. Increasing it further, 4D printing is a new concept in which printed objects respond to environmental stimuli and change shape or other characteristics with time in a controlled and predicted manner. However, the development of bio-based material alternatives that can be integrated into a circular economy is limited if compared with other non-renewable polymers traditionally used for these applications. Bioderived and/or biodegradable thermoplastics reinforced with bioderived fibres have compelling attributes in this context; they can be recycled, can be used in smart materials (4D printing), and, if necessary, can biodegrade at the end of their life cycle, leaving no harmful waste in the environment. In this work, we demonstrate the potential of PLA-based biocomposites with high content of regenerated cellulose fibres (lyocell) for 3D printed structures produced by fused deposition modelling (FDM) that change shape in response to moisture (hygromorphic). The main mechanism involved in this behaviour is related to the anisotropic swelling of the cellulose fibres that are preferentially aligned in the composite during printing. Using a bi-layered architecture of passive and active layers, we developed different prototypes with 2D to 3D transformation capability triggered by moisture with a high degree of shape change.

Keywords: biocomposites; poly lactic acid; 4D printing; shape-change

1. Introduction

Additive manufacturing, or three-dimensional (3D) printing, has demonstrated great potential and has been used in the production of products/parts where customisation is paramount. The wide variety of methods available enables the manufacturing of parts using metals, polymers, ceramics, and composites, achieving different levels of precision and quality. Extrusion-based methods, such as fused deposition modelling (FDM), are the most diffused 3D printing processes used for commercial and DIY applications, especially using thermoplastics and their composites. The ease of such processes and relatively low price of the equipment and materials justify their widespread use [1,2].

Biopolymers, such as polylactic acid (PLA), polyhydroxyalkanoate (PHA), and biobased polybutylene succinate (PBS) are common thermoplastics that can be used for FDM to reduce the environmental impacts associated with materials. Besides being bio-derived and biodegradable, these polymers have the potential to be recycled. The addition of natural fibres as reinforcements also extends the possible use of these polymers, improving the mechanical properties and potentially increasing the biodegradation rate. PLA-based composites are the main materials recently being developed for FDM because of their good combination of processability, printability and mechanical performance [3]. In addition, it has been demonstrated that the intrinsic hydrophilic characteristic of natural fibres, often seen as a problem for the physical performance and application of natural fibre composites, can be used in combination with 3D printing to create hygromorphic structures, e.g. objects that change shape with the variation of moisture, also coined as 4D printing [4–6]. This behaviour is based on the anisotropic swelling, upon

* Corresponding author. Tel.: +64 7 838 4849
E-mail address: cgauss@waikato.ac.nz

water absorption, of cellulose fibres that are aligned during the printing process. If a bilayer structure is used with different swelling/expansion ratios, the structure will curve, as described by the Timoshenko equation [4].

Natural fibres such as wood, hemp, harakeke, and flax, as well as nano cellulose fibres, have been extensively studied and applied for this purpose. However, the natural characteristics of these bio fibres, e.g. heterogeneous surface quality, variation in fibre dimensions, and mechanical properties, often cause problems in the production of filaments for 3D printing. Regenerated cellulose bio fibres can be used to overcome the problems associated with other natural fibres. Lyocell fibres, for example, a type of regenerated cellulose, are produced using N-methyl morpholine-N-oxide (NMMO) in a process named lyocell to dissolve and regenerate cellulose into continuous fibres with uniform and predictable properties. As these fibres are bioderived and produced in a closed system, they are often referred to as a sustainable fibre choice [7,8].

Many studies have demonstrated the potential use of lyocell fibres to improve the overall mechanical properties of PLA composites produced using different manufacturing methods, increasing tensile and flexural strength, modulus of elasticity, elongation at break and impact strength [9–12]. However, the use of these fibres for 3D printing applications has not been explored yet. In this work, we have used lyocell fibres as a reinforcement and as an active material for the production of PLA composites for 3D printing with a focus on 4D printing potential. We have produced filaments with high fibre content (30 wt%) and used them for small-scale FDM printing to explore the hygromorphic properties of this formulation. The same material was then used for larger-scale printing and used to produce a demonstrator of a hygromorphic structure exploring the intrinsic properties of the developed composite.

2. Materials and Methods

2.1. Materials

Poly (lactic acid) (PLA) grade 2003D with melt flow index (MFI) of 6 g/10 min (210°C, 2.16kg) and specific gravity of 1.24 $g.cm^{-3}$ was purchase from NatureWorks®. Stamped lyocell fibres with nominal length of 3 mm were gently provided by Lenzing®, Austria. The fibres have a nominal linear density of 1.7 dtex (equivalent to diameters between 10-12 µm) and a tenacity at break of 35 cN/tex (equivalent to approximately 536 MPa).

2.2. Filament production

The filament composite was produced by melt compounding of PLA with 30 wt% of lyocell fibres. First, PLA and fibres (a total of approximately 2.5 kg) were manually fed into a Labtech 26-44 twin-screw extruder and processed at a temperature profile of 190-210 ºC (from feed zone to extrusion die) and screw speed of 100 rpm. Before extrusion PLA granules were dried at 45 ºC overnight and the fibres were dried at 103 ºC for 24 h. The addition of 30 wt% of relatively long fibres (3 mm) in PLA considerably increases the viscosity of the polymer during extrusion, which limits the mixing efficiency. Therefore, a second extrusion in a smaller twin-screw extruder was necessary. After the first extrusion, the obtained material was granulated into particles of approximately 3 mm in a Moretto GR granulator, dried in a vacuum oven at 60 ºC for 6h and submitted to a second extrusion in a Labtech LTE 20-44 twin-screw extruder at a temperature profile of 170-200 ºC (from feed zone to extrusion die) and screw speed of 40 rpm. After compounding, the obtained material was again granulated into 3 mm particles and processed in Filabot EX2 single screw extruder at 180 ºC. The filament was air-cooled and spooled in a custom-made spooling device synchronised with the extrusion speed to obtain filaments with adequate dimensions. Filaments of 1.75 +/- 0.1 mm were produced for small-scale printing and initial characterisation of the composite and filaments of 2.85 +/- 0.1 mm were produced for large-scale printing.

2.3. Small-scale 3D printing and physical characterisation

In order to evaluate the potential of the lyocell/PLA composites for hygromorphic structures, strips of 80 x 10 x 0.8 mm (LxWxD) were printed in a MakerGear™ M2 desktop 3D printer. These samples were printed with two materials using the parameters given in Table 1: the composite was used for the active layers and neat PLA was used for the passive layers. Layer height was set to 0.2 mm and each of the active and passive layers consisted of 2 layers each. The active layers were printed with a raster angle of 90º and the passive layers were printed with a raster angle of 0º. A representation of the layout used for the bi-material strip is shown in Figure 1. Before printing, the filaments

were vacuum dried at 50 ºC for 2h. After this first experiment, other samples were also 3D printed exploring the same concept, but with different raster angles for the active layer, to validate the potential use of this filament for 4D printing.

Table 1. Parameters used for the 3D printed samples.

Parameter	Value
Infill density	100%
Nozzle diameter	0.75 mm
Bed temperature	50 ºC
Nozzle temperature	210 ºC
Printing speed	1800 mm/min
Layer height	0.2 mm
Active layer raster angle	90º
Passive layer raster angle	0º

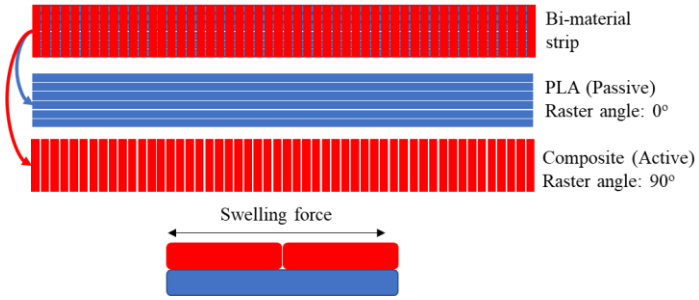

Fig. 1. Representation of the bi-material PLA/Composite strip used for hygromorphic tests.

Once printed, the samples were weighed and soaked in water at room temperature. Their mass was measured after 2h, 24h, 48h, and 165h and the water absorption (%) was determined. The curvature radius was also calculated for each time using the procedure given in Figure 2. The software Image J® was used to analyse the photo and determine the ***c*** and ***d*** dimensions. The experimental curvature was also validated using a modified equation based on Timoshenko's model for thermal expansion in bilayers [13,14], calculated according to Equation 1.

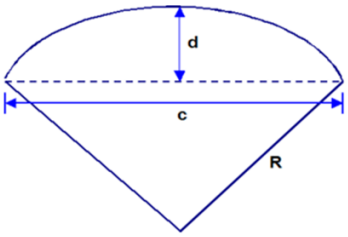

$$R = \frac{c^2 + 4d^2}{8d} \qquad \Delta K = \frac{1}{R}$$

Fig. 2. Representation and equation used to calculate curvature (ΔK).

$$\Delta K = \frac{\Delta\beta \Delta C f(m,n)}{t} \tag{1}$$

$$f(m,n) = \frac{6(1+m)^2}{3(1+m)^2 + (1+mn)(m^2 + \frac{1}{mn})}$$

$$m = \frac{t_p}{t_a} \qquad n = \frac{E_p}{E_a}$$

Where, ΔK is the curvature (1/R), $\Delta\beta$ is the differential of hygroscopic expansion coefficient between active and passive layers; ΔC is the water loss between wet and dry state; t is the total thickness of the sheet; t_p and t_a are the thickness of the passive (PLA) and active (composite) layers, respectively; E_p and E_a are Young's modulus of the passive (PLA) and active (composite) layers, respectively.

2.4. Large-scale 3D printing

The 2.85 mm composite filament was used for a larger-scale printing trial. Flat samples with a bi-material layout (same principle used in the small-scale printing) were printed in a BigRep One ver. 0.3 printer with a build volume of 1 x 1 x 1 m^3 using the parameters given in Table 2. The hygromorphic concept was applied to a flat table design that transforms into a three-dimensional table once immersed in water. The digital design of the table is presented in Figure 3a. To achieve that, the table had to be separated into different parts, so that the central element could keep its shape while the table's legs would bend to an appropriate degree in a way that the table could stand (Figure 3b). For each leg, a unique printing process (and therefore g-code) had to be made, where the printing direction for the active and passive layers is perpendicular and parallel to the bending direction, respectively. For the middle part of the table, the layers of neat PLA and composite were printed with a raster angle of 45/-45º to minimise shape change in this part. After initial trials to adjust and fine-tune the g-code for the BigRep printer (printing only a sample of the table's leg), the active layers using the composite filament were printed first followed by the passive layers, printed with neat PLA.

It is worth mentioning that the intended curve, shown in Figure 3a, would not be possible for thicker samples in a short active segment. In addition, if the active section is too thin, the table would not be structurally stable. Therefore, in order to simplify the printing process and achieve higher curvatures, the entire leg was used as the active part for the shape-changing process, as shown in Figure 3b.

Table 2. Parameters used for the large-scale 3D printing

Parameter	Value
Infill density	100%
Nozzle diameter	1.0 mm
Bed temperature	50 ºC
Nozzle temperature	215 ºC
Printing speed	2400 mm/min
Layer height	0.4 mm

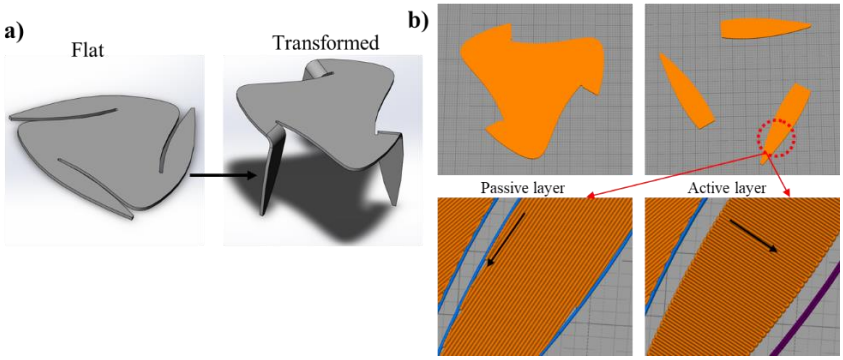

Fig. 3. Table design as flat and after shape change (a); printing process of the active and passive layers and corresponding raster angles in relation to the x-axis (b). The black arrows in (b) indicate the printing direction.

3. Results and Discussion

3.1. Initial trials on 3D printing and shape-changing mechanism

The bi-material strips printed using the filament with 30 wt% of lyocell and neat PLA after different times of immersion in water are shown in Figure 4. It can be observed that after 24 h, the strip already presents a considerable curvature and starts to stabilise within 48 h of immersion. After conditioning the samples in a climatic chamber (CM), the curvature was shown to be reversible, proportionally with the water content. When the samples were stabilised inside a desiccator, the water content dropped to only 0.28%. However, although the samples had a lower water content than after 2h of immersion, the curvature was higher and the sample did not go back to a completely flat state. It is hypothesised, that the strain of neat PLA and matrix involved in the change of curvature was enough to cause permanent/plastic deformation of the polymer.

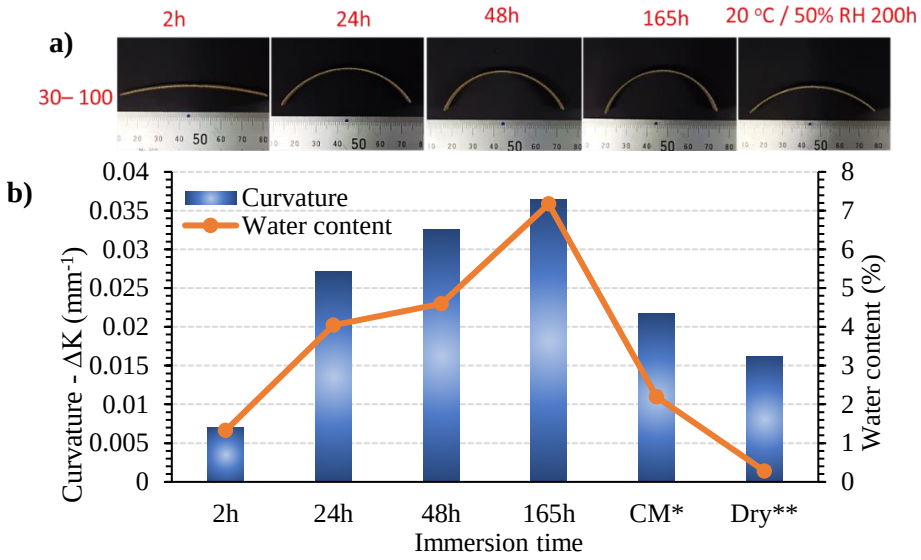

Fig. 4. Pictures of the bi-material strip at different times of immersion in water (a) and corresponding curvature and water content values (b). * CM – Sample conditioned in a climatic chamber at 20ºC / 50% RH for 200h; ** - Samples conditioned in a desiccator at ambient temperature until a constant mass was achieved.

The mechanisms involved in the shape-changing process observed in the samples immersed in water are relatively simple and well described in the literature [3,13,15]. As represented in Figure 5, the layers printed with the composite filament work as the active layer and the layers printed with neat PLA work as a passive layer (with virtually no change with time). Cellulose fibres, including fibres with native cellulose I structure (extracted from plants) and cellulose II structure (regenerated cellulose) in the form of microfibres or nanofibres, are hydrophilic and when in contact with water/moisture, mainly swell in the radial direction with minimal change in length. If fibres in a composite are orientated to a specific direction and the composite is exposed to water, the composite will also swell in the direction perpendicular to the direction of fibre alignment. In the case of printed samples, the swelling will be predominantly perpendicular to the printing direction, as demonstrated in Figure 5a. The orientation of the fibres in printed samples using the lyocell/PLA filaments was verified by X-ray diffraction (XRD) and optical microscopy analyses, confirming that the fibres are aligned with the printing direction, as shown in Figures 5b, and 5c. The swelling of the passive layer printed using neat PLA, can be considered negligible and therefore will restrain the deformation of the active layer, which results in warping/curving of the strip in a direction opposite to the active layer (see Figure 5a), as described by the modified Timoshenko theory [14]. This mechanism was explored for the other printed objects demonstrated in this work.

The change in curvature shown in Figure 4 was also compared with the curvature calculated using the modified Timoshenko equation (Equation 1). The properties used in Equation 1 are given in Table 3. For the active layer, Young's modulus of the composite perpendicular to the printing direction was used and for the passive layer, Young's modulus of neat PLA parallel to the printing direction was used. The coefficient of differential of hygroscopic expansion was determined using samples of 5 x 1.5 x 30 mm^3 3D printed with a filament with 30 wt% of lyocell fibres. By tracking the width swelling and water content of the samples, it was possible to determine the variation of swelling per unit of absorbed water. The swelling and water absorption of neat PLA (used in the passive layer) were negligible if compare with the composite.

Although there are some problems related to the property values used for the calculation of curvature (Young's modulus was not determined for wet/saturated samples), the influence of Young's modulus on the calculated curvature is minimal, considering Equation 1. Figure 6 shows that there is a good agreement between the experimental and calculated, where in both cases, a relatively good correlation factor was obtained using a logarithmic fitting curve.

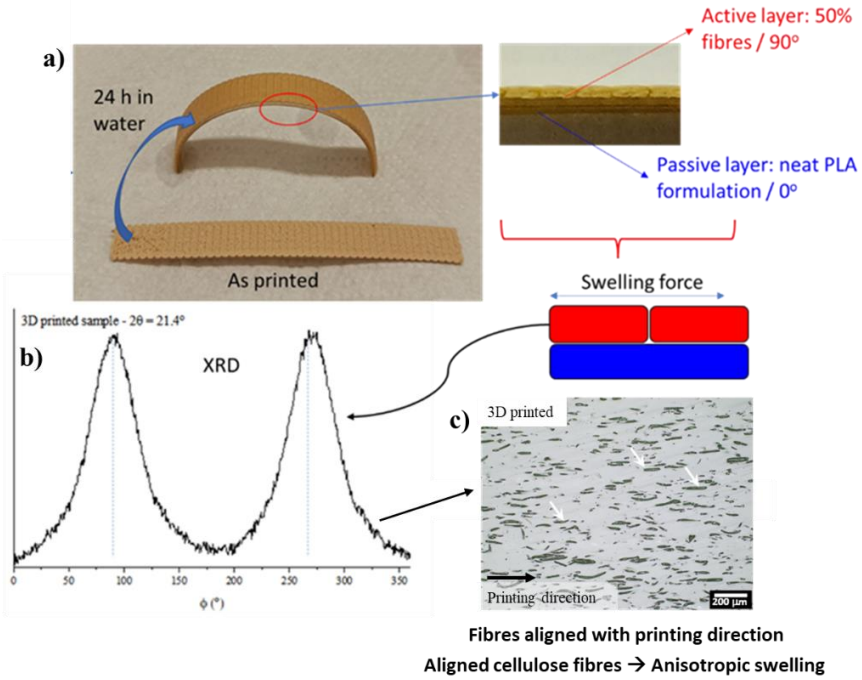

Fig. 5. Mechanism involved in the hygromorphic shape change. The thin strips bend if immersed in water (a) because of the difference in the expansion of active and passive layers. This difference is explained by the presence of aligned cellulose fibres, verified by XRD (b) and optical microscopy (c), that swell mainly in the radial direction. In (c), the fibres are indicated by the white arrows.

Table 3. Properties used to calculate the curvature using the Timoshenko equation.

ID	Parallel to the printing direction (0°) *			Perpendicular to the printing direction (90°) *			$\Delta\beta$** ($\%_s/\%_{wa}$)
	$UTS_{//}$ (MPa)	$E_{//}$ (GPa)	ε_f (%)	$UTS_{\perp}$ (MPa)	$E_{\perp}$ (GPa)	ε_f (%)	
PLA	57.2	3.26	3.96	48.6	3.10	2.22	-
L30%	75.1	6.97	2.50	35.1	3.59	1.11	0.3

* - Tensile test of 3D printed samples (ASTM D638 – type V) using a filament with 30 wt% of lyocell fibres. Number of samples per condition (n) = 5. Testing conditions: cross-head displacement speed: 2mm/min ; 10 mm extensometer; 5 kN loadcell. ** - $\Delta\beta$ is the differential of hygroscopic expansion coefficient. It is described as the percentage of swelling ($\%_s$) per unit of water absoption ($\%_{wa}$). Value obtained by determining the width swelling (perpendicular to the printing direction) and water absorption of samples 3D printed with 30 wt% of lyocell fibres at different immersion times in water. There is no relevant change in the length of the samples.

Obs.: These results were obtained using a filament of a previous study. Although it was not produced according to section 2.2, it is composed of the same polymer and fibre.

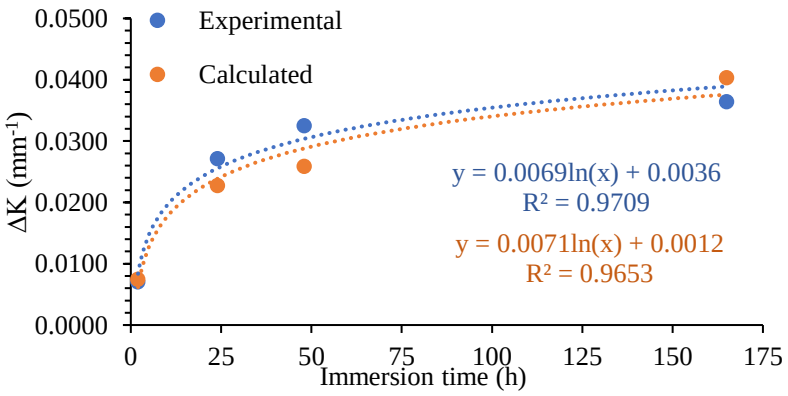

Fig. 6. Comparison between the experimental and calculated curvature values determined using the modified Timoshenko's equation.

The hygromorphic properties of the lyocell/PLA composites were further explored in samples printed with different printing orientations of the active layer. Using the same mechanism described above, not only simple bending movements can be achieved, but also twisting if raster angles of 45º or 60º are used for example. The resulting transformations can be seen in Figure 7. In addition, we accelerated the shape-changing process by increasing the water temperature to 45 ºC. PLA (as the matrix in the composite and as the passive layer) is very sensitive to temperature, and its storage modulus and Young's modulus are greatly affected by the increase in temperature [16]. In this case, the lower modulus of PLA decreases the forces related to swelling of the lyocell fibres necessary for the expansion of the active layer, increasing the degree and rate of shape change. This effect can be visualised in Figure 7 where with only 2h or immersion in water at 45 ºC, the samples are completely "transformed". Even thicker samples were capable of achieving a high degree of shape change.

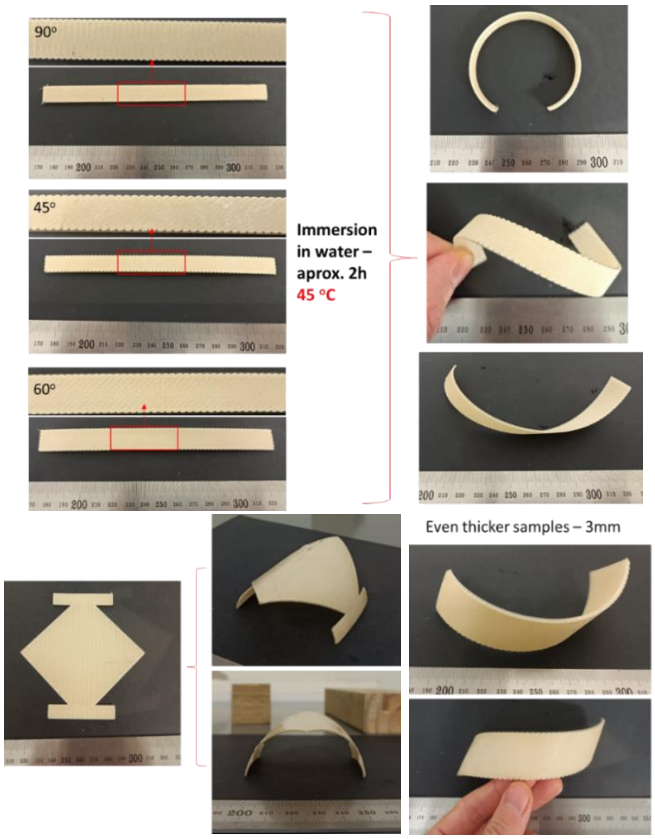

Fig. 7. Other examples of hygromorphic structures using different printing directions of the active layer (90º, 45º, and 60º). The shape-change rate was accelerated by increasing the water temperature.

3.2. Large-scale printing

The large-scale printing was focused on using the flat-pack furniture concept, where we envisage that 4D printing using the hygromorphic transformations can be used to print 2D (flat) furniture that can be self-transformed into three-dimensional furniture only using an external stimulus. In our example, we demonstrated this potential using water immersion, however, depending on the formulation (polymer and fibre content), shape-changing can also be achieved and triggered by the moisture in the environment (although probably much less pronounced).

Before large-scale printing, a small demonstrator was printed using a small printer (the same printer used in the previous examples) with the printing parameters given in Table 1. The active layers were printed first followed by the passive layers. In Figure 8, we demonstrate that the printing strategy was successful and enabled the bending

transformation only on the three legs of the table. The curvature (close to 90º) obtained after transformation was enough to keep the table stable.

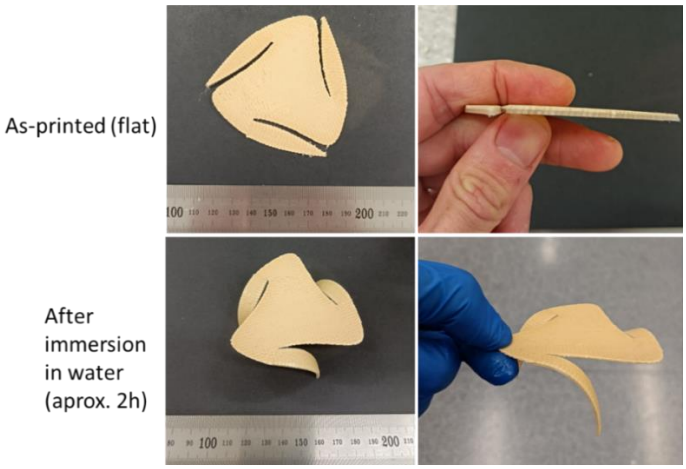

Fig. 8. Initial 3D printing trial of the table design before (flat sample) and after immersion in water at 45 ºC.

Although the table could be successfully printed in a conventional printer, printing on a larger scale brings new challenges in terms of control of parameters, especially when more than one material needs to be printed at different layer heights. Before printing the official table, a few trials were conducted in the BigRep printer to adjust the g-code generated for the table. For these fine adjustments, only the leg was printed since it is the most sensitive part. Figure 9 shows the different attempts (from 1 to 4) necessary to print the bi-material layout. The active layers, printed first, were easily printed using the 1 mm nozzle, without signs of clogging. After finishing these first layers, the composite filament was removed and neat PLA filament was loaded into the printer. However, the values used for the z-axis (height) in the g-code to print the passive layers were not correct, resulting in a lack of contact with the first layers (see Figure 9b on the right). After fine adjustments on the starting z position for the passive layers, the table leg could be printed with both materials without problems (sample L3-4).

After adjusting the g-code for the printer, the final table prototype was printed. Figure 10a shows the printing process with the corresponding raster angles used for each leg. In total, eight different printing processes had to be generated (four for active layers and four for passive layers) that were combined in two steps. In the first step, the active layers were printed using a sequence of four processes (one for each leg and one for the middle part) and in the second step, after changing the filament to neat PLA, the passive layers were printed on the top of the active layers.

The flat table could be successfully printed, taking approximately one hour and forty minutes to finalise both active and passive layers. After printing, the table was immersed in water at room temperature. After approximately 24 h of immersion, it was possible to observe the expected shape-changing effect in the legs of the table, as also visualised in the sample printed in the small printer. However, the obtained curvature was less pronounced, which is explained by the higher thickness of the sample (total of 3.6 mm) and bigger nozzle size (1 mm), which may have reduced fibre alignment, and therefore affected the rate of swelling of the composite used as the active layer. Nevertheless, the transformed table was capable to self-stand and support additional weight.

By adjusting sample design, printing strategy and filament composition, we envisage the use of filaments reinforced with regenerated cellulose fibres extended to large-scale 4D printing of hygromorphic structures, potentially used for furniture and small buildings.

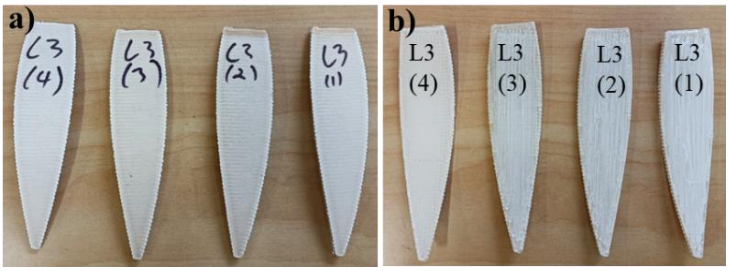

Fig. 10. Initial 3D printing (large-scale) trials to adjust the g-code for bi-material printing at different layer heights for the active (a) and passive (b) layers. First attempt: L3(1); Final attempt (satisfactory): L3(4).

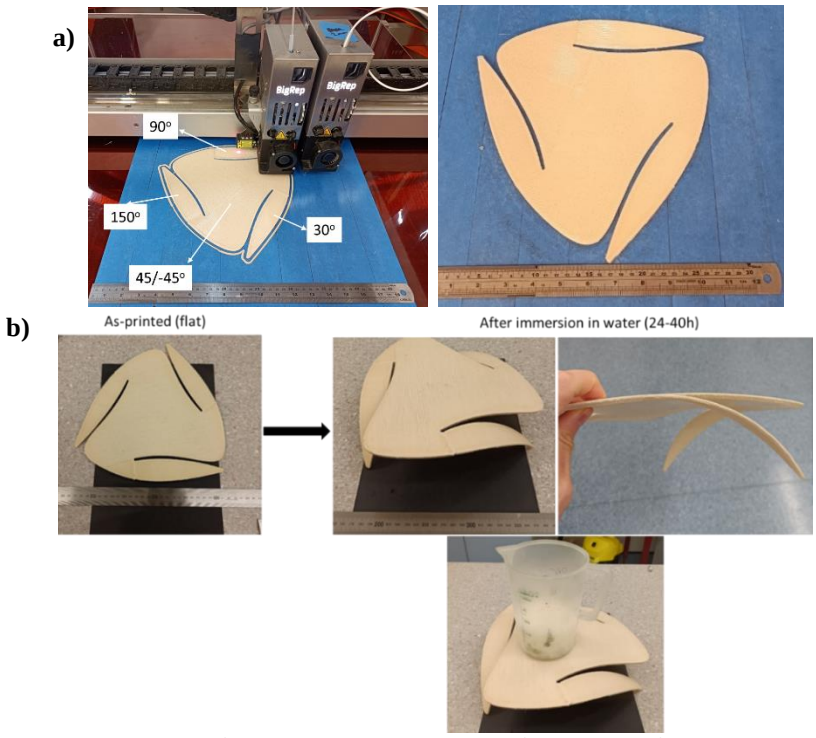

Fig. 10. Printing process and raster angles used for the active layer in each leg and final as-printed flat sample (a). The effect of water immersion on the shape change of the flat table (b).

4. Conclusions

In this work, we demonstrated that lyocell/PLA composites can be used not only for conventional FDM printing but also for 4D printing applications. By exploring the selective alignment of fibres induced by the printing process and the intrinsic anisotropic swelling of the cellulose fibres, hygromorphic structures could be successfully printed with high levels of shape change when the samples are immersed in water. This effect was achieved using a bi-material layout where the developed composite material worked as the active layer and neat PLA was used as a passive layer. The shape-change transformation can be modelled using the Timoshenko equation, which facilitates the design of complex structures. In addition, the lyocell/PLA composite could be processed into filaments for small-scale and large-scale 3D printing, increasing the range of applications for this bio-composite.

By exploring the intrinsic properties of composites with high content of cellulose fibres, this class of material processed by 3D printing can be used in smart systems in the built environment or in the production of furniture with self-assembly characteristics.

Acknowledgements

The authors would like to thank Keith Davis for his valuable help during the large-scale printing. This work received financial support from the Ministry of Business, Innovation and Employment of New Zealand through, National Science Challenge spearhead project “Additive manufacturing and 3D and/or 4D printing of bio-composites’ [grant 2019-S5-CRS].

References

[1] Bi H, Ren Z, Guo R, Xu M, Song Y. Fabrication of Flexible Wood Flour/Thermoplastic Polyurethane Elastomer Composites Using Fused Deposition Molding. Ind. Crops Prod; 2018, 122, p. 76–84, doi:10.1016/j.indcrop.2018.05.059.
[2] Peng Y, Wu Y, Li S, Wang K, Yao S, Liu Z, Garmestani H. Tailorable Rigidity and Energy-Absorption Capability of 3D Printed Continuous Carbon Fiber Reinforced Polyamide Composites. Compos. Sci. Technol; 2020, 199, p. 108337, doi:10.1016/j.compscitech.2020.108337.

[3] Muthe LP, Pickering K, Gauss C. A Review of 3D/4D Printing of Poly-Lactic Acid Composites with Bio-Derived Reinforcements. Compos. Part C Open Access; 2022, 8, p. 100271, doi:10.1016/j.jcomc.2022.100271.
[4] Le Duigou A, Castro M, Bevan R, Martin N. 3D Printing of Wood Fibre Biocomposites: From Mechanical to Actuation Functionality. Mater. Des; 2016, 96, p. 106–114, doi:10.1016/j.matdes.2016.02.018.
[5] Fruleux T, Castro M, Sauleau P, Matsuzaki R, Le Duigou A. Matrix Stiffness: A Key Parameter to Control Hydro-Elasticity and Morphing of 3D Printed Biocomposite. Compos. Part A Appl. Sci. Manuf; 2022, 156, doi:10.1016/j.compositesa.2022.106882.
[6] Correa D, Poppinga S, Mylo MD, Westermeier AS, Bruchmann B, Menges A, Speck T. 4D Pine Scale: Biomimetic 4D Printed Autonomous Scale and Flap Structures Capable of Multi-Phase Movement. Philos. Trans. R. Soc. A Math. Phys. Eng. Sci; 2020, 378, doi:10.1098/rsta.2019.0445.
[7] Zhang S, Chen C, Duan C, Hu H, Li H, Li J, Liu Y, Ma X, Stavik J, Ni Y. Regenerated Cellulose by the Lyocell Process, a Brief Review of the Process and Properties. BioResources; 2018, 13, p. 1–16, doi:10.15376/biores.13.2.Zhang.
[8] Klemm D, Heublein B, Fink H.P, Bohn A. Cellulose: Fascinating Biopolymer and Sustainable Raw Material. Angew. Chemie - Int. Ed; 2005, 44, p. 3358–3393, doi:10.1002/anie.200460587.
[9] Graupner N. Improvement of the Mechanical Properties of Biodegradable Hemp Fiber Reinforced Poly(Lactic Acid) (PLA) Composites by the Admixture of Man-Made Cellulose Fibers. J. Compos. Mater; 2009, 43, p. 689–702, doi:10.1177/0021998308100688.
[10] Graupner N, Müssig J. A Comparison of the Mechanical Characteristics of Kenaf and Lyocell Fibre Reinforced Poly(Lactic Acid) (PLA) and Poly(3-Hydroxybutyrate) (PHB) Composites. Compos. Part A Appl. Sci. Manuf; 2011, 42, p. 2010–2019, doi:10.1016/j.compositesa.2011.09.007.
[11] Baghaei B, Skrifvars M. Characterisation of Polylactic Acid Biocomposites Made from Prepregs Composed of Woven Polylactic Acid/Hemp-Lyocell Hybrid Yarn Fabrics. Compos. Part A Appl. Sci. Manuf; 2016, 81, p. 139–144, doi:10.1016/j.compositesa.2015.10.042.
[12] Graupner N, Ziegmann G, Müssig J. Composite Models for Compression Moulded Long Regenerated Cellulose Fibre-Reinforced Brittle Polylactide (PLA). Compos. Sci. Technol; 2017, 149, 55–63, doi:10.1016/j.compscitech.2017.05.028.
[13] Gladman AS, Matsumoto EA, Nuzzo RG, Mahadevan L, Lewis JA. Biomimetic 4D Printing. Nat. Mater; 2016, 15, p. 413–418, doi:10.1038/nmat4544.
[14] Le Duigou A, Keryvin V, Beaugrand J, Pernes M, Scarpa F, Castro M. Humidity Responsive Actuation of Bioinspired Hygromorph Biocomposites (HBC) for Adaptive Structures. Compos. Part A Appl. Sci. Manuf; 2019, 116, p. 36–45, doi:10.1016/j.compositesa.2018.10.018.
[15] Zolfagharian A, Kaynak A, Bodaghi M, Kouzani AZ, Gharaie S, Nahavandi S. Control-Based 4D Printing: Adaptive 4D-Printed Systems. Appl. Sci; 2020, 10, doi:10.3390/app10093020.
[16] Tábi T, Hajba S, Kovács JG. Effect of Crystalline Forms (α′ and α) of Poly(Lactic Acid) on Its Mechanical, Thermo-Mechanical, Heat Deflection Temperature and Creep Properties. Eur. Polym. J; 2016, 82, p. 232 – 243, doi:10.1016/j.eurpolymj.2016.07.024.